1 H and 13 C NMR Relaxation Studies of Molecular Dynamics of the Thyroid Hormones Thyroxine, 3,5,3‘−Triiodothyronine, and 3,5−Diiodothyronine †

ARTICLE *in* JOURNAL OF MEDICINAL CHEMISTRY · OCTOBER 1996

Impact Factor: 5.45 · DOI: 10.1021/jm960231+ · Source: PubMed

2 AUTHORS, INCLUDING:

Brendan M Duggan
University of California, San Diego
36 PUBLICATIONS **689** CITATIONS

SEE PROFILE

^{1}H and ^{13}C NMR Relaxation Studies of Molecular Dynamics of the Thyroid Hormones Thyroxine, 3,5,3′-Triiodothyronine, and 3,5-Diiodothyronine†

Brendan M. Duggan‡ and David J. Craik*,§

School of Pharmaceutical Chemistry, Victorian College of Pharmacy, Monash University, 381 Royal Parade, Parkville, VIC 3052, Australia, and Centre for Drug Design and Development, University of Queensland, Brisbane, QLD 4072, Australia

Received March 25, 1996⊗

^{1}H and ^{13}C NMR spin−lattice relaxation times and ^{13}C{^{1}H} nuclear Overhauser enhancement factors have been measured for the thyroid hormones thyroxine, 3,5,3′-triiodothyronine, and 3,5-diiodothyronine, with the aim of determining the internal molecular dynamics in these molecules. Spin−lattice relaxation times of protons on the two aromatic rings of these hormones show remarkable differences, with values for the hydroxyl-bearing ring being a factor of 4−12 times larger than those for the alanyl-bearing ring. This difference is not mirrored in the ^{13}C relaxation times, which are identical within experimental error for the two rings. The ^{13}C data show that the mobility of the two rings is similar, and therefore the difference in proton spin−lattice relaxation times arises because the protons of the alanyl-bearing ring are efficiently relaxed by interactions with neighboring protons on the side chain. Quantitative analysis of the ^{13}C relaxation data shows that there must be a significant degree of internal flexibility in the thyroid hormone molecules. The NMR data suggest that in methanol the molecules tumble with an overall correlation time of approximately 0.35 ns, but that rapid internal motion (in the form of jumps between two stable conformations) occurs on a 30-fold faster time scale. When combined with previous variable temperature NMR studies that show interconversion between proximal and distal forms of the outer ring on the microsecond time scale, the results provide a complete description of the conformations and both fast and slow internal motions in the thyroid hormones. The findings suggest that modeling studies of thyroid hormone interactions with receptor proteins should take into account the possibility that these internal motions are present. In effect, the thyroid hormones may likely populate a larger range of conformations in the bound state than might be inferred from just the lowest energy forms seen in the crystal and solution states.

Introduction

The thyroid hormones thyroxine (T4) and 3,5,3′-triiodothyronine (T3) are important in the regulation of a wide range of metabolic processes. They are synthesized in the thyroid gland, circulate in the bloodstream bound to various transport proteins, and exert their action on target cells following binding to nuclear receptor proteins.[1−3] There have been many studies on the relationship between structure and activity of the hormones,[4−6] but the precise molecular interactions involved in their biological action remain unknown. A full understanding of their interaction with transport proteins and the nuclear receptor requires a knowledge of their conformations. X-ray crystallographic studies have provided much information on the solid state,[1] and aspects of their solution conformations have been determined by NMR spectroscopy.[7−9] As the hormones are potentially flexible molecules, it is also important to have an understanding of their internal molecular dynamics as well as their conformation. In the current paper this is achieved by measurements of NMR spin−lattice relaxation times (T_1) and nuclear Overhauser enhancement (NOE) factors.

The basic hormone structure consists of an iodinated diphenyl ether moiety and an alanyl side chain. The aromatic ring attached to the alanyl side chain is often referred to as the "inner" ring and the second phenyl group which contains a para hydroxyl group, as the "outer" ring.[1] The degree of iodination affects the binding and activity of the hormone, with T3 being approximately 10-fold more active than T4. A range of other thyroid hormones, with reduced activity, are also found in the body, for example, 3,3′,5′-triiodothyronine (rT3) and 3,5-diiodothyronine (T2).

In solution, and in the solid state, the hormones generally adopt a conformation in which the two aromatic rings are roughly perpendicular to one another,[10−13] as illustrated in Figure 1. Knowledge of this three-dimensional shape provides a starting point for modeling the interactions of the hormones with their target proteins, but the representation shown in Figure 1a is somewhat simplified, because it is known that there are significant dynamic motions associated with the outer ring. Studies on soluble analogues,[8,14] and later on T4 and T3 themselves,[9] have shown that rotation about the diphenyl ether linkage with a barrier of approximately 36 kJmol^{-1} produces an interchange of the environment of H2′ with that of H6′. For hormones which are symmetrically iodinated in the outer ring, the interchange occurs between isoenergetic (and structurally

† Abbreviations: T4, thyroxine; T3, 3,5,3′-triiodothyronine; T2, 3,5-diiodothyronine; T_1, spin−lattice relaxation time; T_2, spin−spin relaxation time; NOE, nuclear Overhauser enhancement.

* Author to whom correspondence should be addressed. E-mail: d.craik@mailbox.uq.oz.au.

‡ Victorian College of Pharmacy.

§ University of Queensland.

⊗ Abstract published in *Advance ACS Abstracts,* August 15, 1996.

S0022-2623(96)00231-2 CCC: $12.00

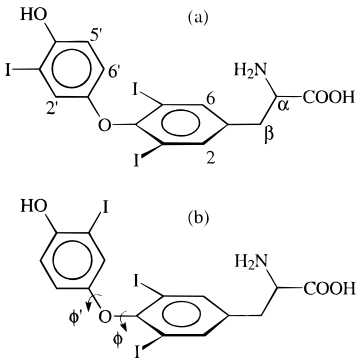

Figure 1. Conformations of thyroid hormones. (a) A representation of the conformation of T3 found in the crystal structure.[11] This is the distal form in which the outer ring iodine points away from the inner ring. (b) The proximal form showing the torsion angles ϕ and ϕ' that define the diphenyl ether conformation. The conformation in solution is similar to these in that the two rings are mutually perpendicular. In principle, each conformation leads to a considerable difference in the ^{1}H NMR chemical shifts of the outer ring protons H2′ and H6′ due to ring current effects from the inner ring. In practice, at room temperature rapid rotation about the diphenyl ether bonds results in averaging of the two chemical shifts, i.e. proximal and distal forms are readily interconverted in solution. Below 185 K the separate conformers can be detected in solution at 300 MHz.

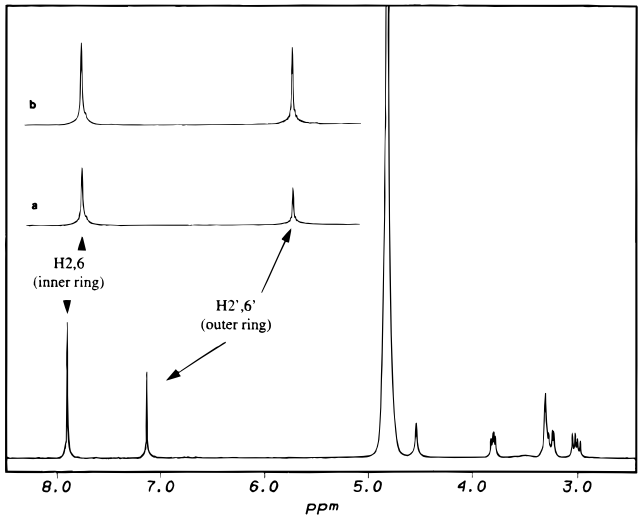

Figure 2. 300 MHz ^{1}H NMR spectrum of T4 in methanol-d_4 at 306.5 K showing the difference in intensity of the two aromatic resonances that suggests different relaxation rates for the two resonances. The relaxation delay between scans was 1 s. The inset shows expanded sections of the aromatic region: (a) relaxation delay = 1 s, (b) relaxation delay = 5 s. The expansion shows that the line widths of the two aromatic signals are similar. The intensities are similar in part b, but at shorter relaxation delays, the inner ring signal is reduced in intensity due to relaxation effects.

equivalent) forms, but for monoiodinated derivatives such as T3, the rotation about the diphenyl ether linkage interconverts "proximal" and "distal" forms of the hormone, as illustrated in Figure 1. Studies based on sterically constrained analogues have suggested that the distal form is more active,[15] and indeed this appears to be the conformation in which the hormone binds to the receptor.[16]

In previous studies we have examined the conformational properties of the thyroid hormones using NMR spectroscopy[9,17] and have used theoretical calculations to examine the potential mechanisms for interconversion of outer ring environments.[18] In the course of the NMR studies it was noted that in the 300 MHz ^{1}H NMR spectrum of T4, the signal intensity of the H2′,6′ protons is generally lower than that of the H2,6 protons. As the line widths of the peaks are similar (see Figure 2), this suggests a difference in the spin−lattice relaxation times of the two pairs of protons. NMR relaxation times depend on both molecular mobility and dipolar interactions of a given nucleus with neighboring protons, and so the observed difference could arise from either a difference in the relative mobility of the inner and outer rings or from differential interactions of the inner ring protons with other protons in the alanyl side chain. To discriminate between these possibilities, and to examine in detail the molecular mobility of the thyroid hormones, a series of ^{1}H and ^{13}C NMR relaxation time measurements has been made for T4, T3, T2, and T4 sodium salt in methanol and for T4 in DMSO. These solvents were chosen so as to provide a range of solution viscosities and because the hormones are sparingly soluble in aqueous solution. Given that previous variable temperature NMR studies have shown that the outer ring undergoes dynamic motion on the microsecond time scale, it was of interest to see whether this ring undergoes additional motion that could be detected by relaxation time measurements.

The study of internal molecular motion in bioactive species is of significant interest because a knowledge of the rate and amplitude of motions in solution places limits on conformations which may be expected in the bound state. In some cases conformational changes may occur in the bound state. For example studies of the dihydrofolate reductase−methotrexate complex have found that the ligand exhibits dynamic flexibility when bound.[19−21] While a relationship between dynamics and flexibility has yet to be established in the general case of drug−receptor interactions, it is reasonable to propose that, at least in some cases, ligand flexibility at the bound site may contribute to receptor activation. In addition, ligands which display a significant degree of internal flexibility in solution might be expected to exhibit an unfavorable entropic contribution to binding relative to more rigid ligands, and therefore methods for examining internal flexibility in solution have potential application in drug design.

Molecular dynamics of the thyroid hormones are of particular interest following the recent publication of several crystal structures of nuclear receptor ligand-binding domains. Crystal structures of the thyroid receptor,[16] retinoic acid receptor,[22] and retinoid-X receptor[23] ligand binding domains show that the long identified sequence similarity[24] leads to highly homologous folds of the proteins. The bound and free forms of the nuclear receptor ligand binding domains demonstrate that ligand binding induces a significant conformational change in the protein, trapping the ligand at its center.

Results

Figure 2 shows the 300 MHz ^{1}H NMR spectrum of T4 recorded with a 1 s relaxation delay between radiofrequency pulses in a Fourier transform NMR experiment. The difference in intensity of the signals from the inner and outer rings is readily apparent. The inset on Figure 2 shows an expansion of the aromatic region

Table 1. ^1H Relaxation Times and Chemical Shifts of the Protons of T4, T3, and T2 in Methanol[a]

	^1H T_1[b] (s)			chemical shift (ppm)		
	T4	T3	T2	T4	T3	T2
H2′	8.36 ± 0.39	1.64 ± 0.16	1.38 ± 0.10	7.13	7.05	6.58
H3′	*c*	*c*	1.99 ± 0.13	*c*	*c*	6.69
H5′	*c*	1.69 ± 0.12	1.99 ± 0.13	*c*	6.74	6.69
H6′	8.36 ± 0.39	0.96 ± 0.11	1.38 ± 0.10	7.13	6.63	6.58
H2,6	1.60 ± 0.08	0.15 ± 0.01	0.28 ± 0.08	7.90	7.88	7.86
Hα	0.91 ± 0.09	0.04 ± 0.00	0.10 ± 0.04	3.79	3.77	3.74
Hβ	0.34 ± 0.06	0.09 ± 0.07	0.16 ± 0.06	3.25	3.23	3.21
Hβ'	0.31 ± 0.04	0.06 ± 0.01	0.13 ± 0.04	3.00	2.99	2.97

[a] Data were obtained at 306.5 K and 300 MHz using saturated solutions (~1 mM) of the free acid in methanol-d_4. [b] Values are the average ± standard deviation of eight (T4), four (T3), or six (T2) T_1 experiments. [c] This position carries an iodine atom rather than a proton signal.

of the T4 spectra recorded with relaxation delays of 1.0 and 5.0 s. The relative saturation of the inner ring protons at the shorter relaxation delay is readily apparent. This suggests that the intensity difference arises from effects of the spin−lattice relaxation time (T_1), rather than the spin−spin relaxation time (T_2), an observation confirmed by the similarity in line widths of the two signals. Similar observations were also made for two other thyroid hormones, 3,5,3′-triiodothyronine (T3) and 3,5-diiodothyronine (T2).

To quantitate the magnitude of the T_1 difference, a series of inversion recovery ^1H T_1 experiments was recorded, and the results are summarized in Table 1. Also shown in the table are ^1H chemical shifts in methanol which are in close agreement with values previously reported in DMSO.[25] In general, T_1s for the side chain protons are smallest, followed by those for the inner ring, with the outer ring T_1s being significantly larger. The difference between T_1s of the inner and outer rings is quite marked, with the outer ring T_1s being greater by a factor of between 4 and 12 for the three hormones. For T4, for example, the outer ring T_1 is 8.4 s and the inner ring T_1 is 1.6 s.

To determine if this difference in the ^1H T_1s is related to differing relative motion of the two rings, or due to contributions to relaxation of the inner ring protons by the side chain protons, ^{13}C relaxation time measurements were made. Such measurements are less susceptible to external influences, including dissolved oxygen, than proton T_1s and are normally dominated by dipole−dipole relaxation with the attached proton. One difficulty with these measurements is the extremely low solubility of the thyroid hormones in aqueous media, resulting in low signal-to-noise for natural abundance ^{13}C spectra. Measurements were therefore not possible in aqueous solution and were instead recorded in methanol. The derived T_1s for T4, T3, and T2 are given in Table 2, along with corresponding $^{13}C\{^1H\}$ NOEs and chemical shifts. The ^{13}C chemical shifts of T3 are in good agreement with values reported for the hormone in DMSO.[26]

In sharp contrast with the ^1H relaxation times, the ^{13}C T_1s for the two rings of all three of the thyroid hormones are identical within experimental error. For T4, for example, the values for the inner and outer rings are both 0.63 s. This strongly suggests that the motion of the two rings is similar. This is confirmed by the $^{13}C\{^1H\}$ NOE data in Table 2. For the hydrogen-bearing carbons, NOE values are similar for the two rings. The observed difference in ^1H T_1 values for the two rings therefore reflects the additional intramolecular contribution to relaxation of the inner ring protons from the side chain.

The above qualitative analysis of relaxation data shows that the two aromatic rings have similar mobilities. It is now of interest to quantitatively determine the parameters describing motion in the hormones and to determine the nature of any internal motions. Equations 1 and 2[27] show the relationship between the relaxation parameters (T_1 and NOE) and motional parameters, which are incorporated into the spectral density function $J(\omega)$. These equations assume exclusively dipolar relaxation, where N is the number of protons attached to the observed ^{13}C nucleus, the γ- and ω-terms represent the gyromagnetic ratios and Larmor frequencies of the ^{13}C and ^1H nuclei involved in the dipole−dipole interaction, r_{CH} is their internuclear separation, and $\hbar$ is Planck's constant divided by 2π.

$$\frac{1}{NT_1} = \frac{1}{10}\left(\frac{\gamma_C^2\gamma_H^2\hbar^2}{r_{CH}^6}\right)[J(\omega_H - \omega_c) + 3J(\omega_c) + 6J(\omega_H + \omega_c)] \quad (1)$$

$$\mathrm{NOE} = 1 + \frac{\gamma_H}{\gamma_X}\left(\frac{6J(\omega_H + \omega_X) - J(\omega_H - \omega_X)}{J(\omega_H - \omega_X) + 3J(\omega_H) + 6J(\omega_H + \omega_X)}\right) \quad (2)$$

The spectral density term $J(\omega)$ conveniently describes the frequency and orientational components of motion (more formally defined as the Fourier transform of the orientational and autocorrelation function). For the practical use of eqs 1 and 2, it is necessary to have an explicit mathematical formulation of spectral density which is in turn dependent on the model chosen to represent motion present in the molecule. The simplest model for molecular motion is that of a rigid C−H vector

Table 2. ^{13}C T_1s, $^{13}C\{^1H\}$ NOEs, and Chemical Shifts of the Hydrogen-Bearing Carbons of T4, T3, and T2 in Methanol[a]

	^{13}C T_1[b] (s)			$^{13}C\{^1H\}$ NOE[c]			chemical shift (ppm)		
	T4	T3	T2	T4	T3	T2	T4	T3	T2
C2′	0.63 ± 0.10	0.64 ± 0.17	0.65 ± 0.11	2.53 ± 0.38	2.58 ± 0.55	2.41 ± 0.22	127.3	126.8	117.4
C3′	*d*	*d*	0.88 ± 0.11	1.28 ± 0.20	1.48 ± 0.25	2.50 ± 0.27	85.5	84.4	116.9
C5′	*d*	0.79 ± 0.19	0.88 ± 0.11	1.28 ± 0.20	2.67 ± 0.50	2.50 ± 0.27	85.5	115.9	116.9
C6′	0.63 ± 0.10	0.63 ± 0.22	0.65 ± 0.11	2.53 ± 0.38	2.91 ± 0.44	2.41 ± 0.22	127.3	117.7	117.4
C2,6	0.63 ± 0.09	0.80 ± 0.11	0.70 ± 0.18	2.63 ± 0.37	2.35 ± 0.42	2.55 ± 0.27	142.6	142.5	142.4
Cα	0.51 ± 0.14	0.56 ± 0.10	0.65 ± 0.15	2.37 ± 0.64	2.28 ± 0.55	2.24 ± 0.42	57.1	57.2	57.2
Cβ	0.64 ± 0.18	0.86 ± 0.14	0.88 ± 0.06	2.29 ± 0.68	2.38 ± 0.56	2.10 ± 0.22	36.4	36.6	36.5

[a] Data were obtained at 306.5 K and 75 MHz using saturated solutions (~1 mM) of the free acid in methanol-d_4. [b] Values are the average ± standard deviation of four T_1 experiments. [c] Values are the average ± standard deviation of five (T4), four (T3), and four (T2) NOE experiments. [d] Atom is iodinated rather than protonated.

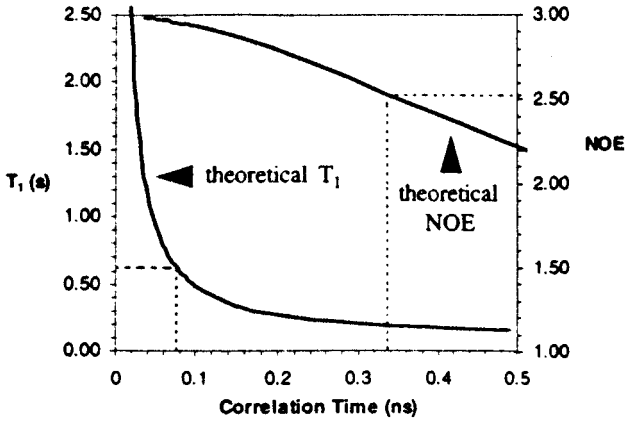

Figure 3. Experimental ^{13}C T_1 and $^{13}C\{^1H\}$ NOE values for T4 are shown superimposed onto theoretical plots for the isotropic diffusion model. The solid lines represent the T_1 and NOE values predicted by the isotropic diffusion model (eqs 1−3). The dotted lines represent the experimental values obtained for the outer ring protons of T4 ($T_1 = 0.63$ and NOE = 2.53) and the correlation times they correspond to. For the model to satisfy the data, the experimental T_1 and NOE should give the same correlation time. Clearly, the isotropic diffusion model does not do this.

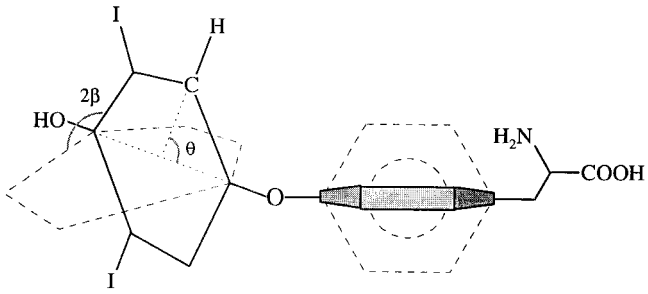

Figure 4. Definition of the angles and states of the two state jump model as applied to thyroxine. For clarity the angles are shown only for the outer ring, but the inner ring also undergoes the jumping motion. The two state jump model describes the motion of a CH vector attached to a molecule tumbling with overall correlation time, τ_o and undergoing an internal conformational jump between two discrete states. The two different conformations are separated by a half jump angle, β. The rate of jumping between the two states is defined by τ_i, the lifetime of each state (assumed to be equal for the two conformers). The CH vector makes an angle, θ, with the jump axis. The alternate conformations of the aromatic rings are shown as dashed lines.

attached to a molecule tumbling isotropically in solution. In this case, the only motional term is τ, the correlation time for molecular tumbling, and the spectral density function takes the form

$$J(\omega) = \frac{\tau}{1 + \omega^2\tau^2} \tag{3}$$

For more complicated motions, additional correlation times and geometric factors need to be included in the spectral density function. Many of the spectral density functions for various motional models are conveniently incorporated into the program MOLDYN,[28] which was used for analysis of the NMR data in this study. The program includes an iterative fitting routine to determine the set of motional parameters which leads to the best match of theoretical and experimental relaxation parameters for a user-chosen model of molecular motion.

Figure 3 shows an attempt to fit the ^{13}C NMR relaxation data for T4 to the motional model of a rigid molecule tumbling isotropically in solution. The figure shows that it is not possible to simultaneously fit the T_1 and NOE data; i.e., there is no single correlation time which satisfactorily accounts for the relaxation data in this molecule. This shows that motion is more complicated than simple isotropic tumbling. Attempts to fit the data to a model involving overall anisotropic motion of a rigid molecule were similarly unsuccessful. In this case iterative fits which allowed up to a 100-fold degree of anisotropy of principle diffusion coefficients (the largest anisotropy that could reasonably be expected for an organic molecule of this size) did not provide a good fit to the data. Thus, the experimental data clearly show that some degree of internal mobility must be present in the thyroid hormones.

A number of spectral density functions incorporating internal motion have previously been formulated, ranging from those incorporating internal diffusion of rotatable groups to jump models in which rapid flips occur between defined conformations.[29−36] For any of these models, an examination of the appropriate spectral density functions makes it clear that slow internal motions, i.e., those on the millisecond time scale, do not contribute significantly to T_1 and NOE values. Our previous studies of NMR line shape as a function of temperature[9] have shown that large scale rotations of the outer ring of T4 and T3, which result in interconversion of H2′ and H6′, occur on a millisecond to microsecond time scale. Relative to the motions detected by NMR relaxation measurements, however, this is still slow and will have very little influence on the experimentally determined relaxation parameters. To account for the experimental results, faster internal motion must also be present.

Considering the structure of the thyroid hormones, it seems most likely that any rapid internal motions which contribute to the observed relaxation data will occur as small amplitude jumps between discrete states, rather than continuous internal diffusion. The experimental data were therefore fitted to the model described by London[32] for a two-state jump superimposed on overall isotropic motion. This model has successfully been applied to account for differences in relaxation times due to conformational jumps, both in proteins[32] and in organic molecules.[33] The angles used in this model are shown in Figure 4 superimposed on one of the rings of thyroxine, but both rings potentially undergo similar motions, and the angles are defined in the same way. In this model, τ_o is the overall correlation time, θ is the angle between individual CH vectors and the jump axis, β is the half-angle of the jump, and τ_i is the lifetime of individual conformers (hereafter referred to as the internal correlation time to facilitate comparison with other models). For the ring atoms of all the thyroid hormones, β is defined by the geometry of the molecule and is fixed at 60° while, in principle, the other parameters are variable. There is no reason to favor one jump conformer over the other; therefore, the lifetimes of the two states were assumed to be equal.

Fits to the two state jump model were compared with those of the simple isotropic model and with those of the so-called "model-free approach".[37,38] In the latter approach motion is described by an overall correlation time, τ_c, an internal correlation time, τ_i, and an order

Table 3. Theoretical ^{13}C T_1s and $^{13}C\{^1H\}$ NOEs Fitted to T4 in Methanol Data

Isotropic Motion

	^{13}C T_1 (s)	$^{13}C\{^1H\}$ NOE	R (%)	τ_o (ns)
C2′,6′	0.63	2.96	8.7	0.08
C2,6	0.63	2.96	6.4	0.08
Cα	0.51	2.94	12.5	0.10
Cβ	0.64	2.96	15.0	0.07

Two-State Jump

	^{13}C T_1 (s)	$^{13}C\{^1H\}$ NOE	R (%)	τ_o (ns)	τ_i (ns)	β	θ
C2′,6′	0.63	2.53	0.0	0.35[a]	0.01	47	60[a]
C2,6	0.63	2.58	1.1	0.35[a]	0.03	55	60[a]
Cα	0.51	2.51	3.0	0.35[a]	< 0.01	40	60[a]
Cβ	0.64	2.51	4.8	0.35[a]	< 0.01	42	109.5[a]

Model-Free Approach

	^{13}C T_1 (s)	$^{13}C\{^1H\}$ NOE	R (%)	τ_o (ns)	τ_i (ns)	S
C2′,6′	0.63	2.53	0.0	0.50[a]	0.04	0.38
C2,6	0.63	2.63	0.0	0.50[a]	0.05	0.34
Cα	0.51	2.37	0.0	0.50[a]	0.03	0.49
Cβ	0.64	2.29	0.0	0.50[a]	0.01	0.47

[a] This parameter was fixed during iterative fitting.

parameter, S. This approach does not presuppose a specific geometric model for the internal motion but makes the assumption that it is restricted in amplitude (as measured by the order parameter). It was examined here because it has been widely applied to the study of internal motions in cases where it is not necessarily clear what the nature of the internal motion might be, e.g. in proteins where multiple internal motions of differing amplitudes and rates are present. One potential difficulty in the application of a highly specific model to thyroxine (e.g. the two state jump model described above), is that the nature of the internal motion is unknown. Is it reasonable to model the central ether oxygen as the "core" of the molecule upon which is superimposed jumps for each of the two rings and additional motions for the side chain? Because of this uncertainty, it was felt reasonable to compare the simple isotropic model (no internal motion) with a highly specific model (the two state jump model) and with the model-free approach.

Tables 3, 4, and 5 summarize the fits to the various models for T4, T3, and T2, respectively. For each of the hydrogen-bearing carbon sites they show the motional parameters derived from each of the three models by iteratively fitting the theoretically predicted relaxation parameters to the experimental values in Table 2. It is convenient to compare the quality of the fit by calculating a parameter, R, which is a measure of the average deviation of experimental versus fitted parameters, where n is the number of parameters, expressed as a percentage.

$$R = \frac{1}{n}\sum\sqrt{\left(\frac{\text{expt} - \text{theory}}{\text{expt}}\right)^2} \qquad (4)$$

An R value of 0% represents exact agreement of the experimental and theoretical values.

An R factor of 10% or more is obtained for most of the fits of the isotropic motion model to the T4, T3, and T2 data. The fit is improved significantly by the introduction of internal motion. Both the two state jump model and the model-free approach improve the fit for all the ring atoms. Of the fits to the two state jump model, only C6′ and C2,6 of T3 and C3′,5′ of T2 yield R factors greater than 2.5%. This is a significant improvement and shows that models which incorporate internal motion are more appropriate than those which lack such motion.

It is important to establish that any improvement to the fit is not simply due to an increase in the number

Table 4. Theoretical ^{13}C T_1s and $^{13}C\{^1H\}$ NOEs Fitted to T3 in Methanol Data

Isotropic Motion

	^{13}C T_1 (s)	$^{13}C\{^1H\}$ NOE	R (%)	τ_o (ns)
C2′	0.65	2.96	7.5	0.07
C5′	0.79	2.97	5.7	0.06
C6′	0.63	2.96	0.9	0.08
C2,6	0.80	2.97	13.4	0.06
Cα	0.55	2.95	15.2	0.09
Cβ	0.86	2.97	12.6	0.05

Two-State Jump

	^{13}C T_1 (s)	$^{13}C\{^1H\}$ NOE	R (%)	τ_o (ns)	τ_i (ns)	β	θ
C2′	0.64	2.61	0.6	0.30[a]	< 0.01	41	60[a]
C5′	0.80	2.61	1.6	0.30[a]	< 0.01	53	60[a]
C6′	0.63	2.69	4.2	0.30[a]	0.05	55	60[a]
C2,6	0.80	2.61	5.7	0.30[a]	< 0.01	55	60[a]
Cα	0.44	2.62	17.8	0.30[a]	0.02	78	60[a]
Cβ	0.80	2.61	8.5	0.30[a]	< 0.01	49	109.5[a]

Mode-Free Approach

	^{13}C T_1 (s)	$^{13}C\{^1H\}$ NOE	R (%)	τ_o (ns)	τ_i (ns)	S
C2′	0.64	2.58	0.0	0.50[a]	0.04	0.36
C5′	0.79	2.67	0.0	0.50[a]	0.04	0.28
C6′	0.63	2.91	0.0	0.50[a]	0.08	0.13
C2,6	0.80	2.35	0.0	0.50[a]	0.01	0.40
Cα	0.56	2.28	0.0	0.50[a]	0.02	0.50
Cβ	0.86	2.38	0.0	0.50[a]	0.01	0.37

[a] This parameter was fixed during iterative fitting.

Table 5. Theoretical ^{13}C T_1s and $^{13}C\{^1H\}$ NOEs Fitted to T2 in Methanol Data

Isotropic Motion

	^{13}C T_1 (s)	$^{13}C\{^1H\}$ NOE	R (%)	τ_o (ns)
C2′,6′	0.65	2.96	11.7	0.07
C3′,5′	0.88	2.97	9.5	0.05
C2,6	0.70	2.96	8.2	0.07
Cα	0.65	2.96	16.5	0.07
Cβ	0.88	2.97	21.0	0.05

Two-State Jump

	^{13}C T_1 (s)	$^{13}C\{^1H\}$ NOE	R (%)	τ_o (ns)	τ_i (ns)	β	θ
C2′,6′	0.65	2.51	2.1	0.35[a]	< 0.01	47	60[a]
C3′,5′	0.73	2.51	8.7	0.35[a]	< 0.01	55	60[a]
C2,6	0.70	2.53	0.5	0.35[a]	0.01	55	60[a]
Cα	0.65	2.51	6.0	0.35[a]	< 0.01	64	60[a]
Cβ	0.73	2.51	18.3	0.35[a]	< 0.01	49	109.5[a]

Mode-Free Approach

	^{13}C T_1 (s)	$^{13}C\{^1H\}$ NOE	R (%)	τ_o (ns)	τ_i (ns)	S
C2′,6′	0.65	2.41	0.0	0.50[a]	0.02	0.42
C3′,5′	0.88	2.50	0.0	0.50[a]	0.02	0.33
C2,6	0.70	2.55	0.0	0.50[a]	0.04	0.35
Cα	0.65	2.41	3.8	0.50[a]	< 0.01	0.48
Cβ	0.88	2.41	7.4	0.50[a]	< 0.01	0.42

[a] This parameter was fitted during iterative fitting.

Table 6. ^{13}C T_1s and $^{13}C\{^1H\}$ NOEs of the Hydrogen-Bearing Aromatic Carbons of T4, Sodium Salt, in Methanol[a]

	^{13}C T_1 (s)[b]		$^{13}C\{^1H\}$ NOE[c]		chemical shifts
	75 MHz	125 MHz	75 MHz	125 MHz	(ppm)
C2′,6′	0.477 ± 0.010	0.459 ± 0.012	2.15 ± 0.05	2.10 ± 0.06	126.9
C2,6	0.415 ± 0.039	0.462 ± 0.004	2.27 ± 0.10	2.27 ± 0.09	142.3

[a] Data were obtained at 306.5 K using a saturated solution (~10 mM) of the salt in methanol-d_4. [b] Values are the average ± standard deviation of six (75 MHz) and two (125 MHz) T_1 experiments. [c] Values are the average ± standard deviation of three NOE experiments.

Table 7. Theoretical ^{13}C T_1s and $^{13}C\{^1H\}$ NOEs Fitted to T4, Sodium Salt, in Methanol Data

Isotropic Motion

	^{13}C T_1 (s)		$^{13}C\{^1H\}$ NOE			
	75 MHz	125 MHz	75 MHz	125 MHz	R (%)	τ_o (ns)
C2′,6′	0.21	0.54	1.17	1.16	41.1	5.99
C2,6	0.21	0.54	1.17	1.16	41.2	6.05

Two-State Jump

	^{13}C T_1 (s)		$^{13}C\{^1H\}$ NOE						
	75 MHz	125 MHz	75 MHz	125 MHz	R (%)	τ_o (ns)	τ_i (ns)	β	θ
C2′,6′	0.39	0.51	2.22	2.06	8.6	0.70[a]	0.10	55	60[a]
C2,6	0.38	0.49	2.25	2.09	5.8	0.70[a]	0.11	55	60[a]

Model-Free Approach

	^{13}C T_1 (s)		$^{13}C\{^1H\}$ NOE					
	75 MHz	125 MHz	75 MHz	125 MHz	R (%)	τ_o (ns)	τ_i (ns)	S
C2′,6′	0.41	0.51	2.34	2.22	10.1	0.70[a]	0.06	0.45
C2,6	0.39	0.49	2.36	2.25	4.0	0.70[a]	0.07	0.45

[a] This parameter was fixed during iterative fitting.

of variable parameters. While there are three variables per carbon site for both the two state jump and the model-free approaches (θ is effectively a fixed variable in the former model), the fact that four sites were sampled, and that each must have the same value for τ_o, reduces the number of variable parameters per site to two (i.e. τ_i and β for the two state jump model and τ_i and S for the model-free approach), compatible with the experimental points per carbon atom. The fits in Tables 3−5 to the models incorporating internal motion were achieved by initially allowing all the parameters to vary and then fixing τ_o at the average value obtained in the initial fit and iteratively fitting the remaining variable parameters.

To further verify that incorporation of internal motion was necessary to improve the fits, the field dependence of the relaxation parameters was investigated. Consideration of eqs 1 and 2 shows that NMR relaxation parameters may be field dependent, depending on the motional regime present. Therefore, a useful means of testing the applicability of a model of motion is measurement of relaxation parameters at two different field strengths. This in effect doubles the number of experimental data points per carbon site (i.e. two NOE and two T_1 measurements yields four data points per site, with only two or three fitted variables in each model), but more importantly, provides a stringent test of the validity of a particular motional model.

The sodium salt of T4 was used to obtain relaxation data at two different fields (75 and 125 MHz) as it is more soluble than the free acid, therefore improving the signal to noise. It was also of interest to determine the effect of charge state on mobility by comparing the data for the salt with that of the free acid. Table 6 shows the ^{13}C T_1, NOE, and chemical shift data for the sodium salt of thyroxine. Interestingly, under the conditions studied there is not a significant field dependence of either T_1 or NOE values.

The three models used previously, isotropic motion, the two state jump model, and the model-free approach were all fitted to the experimental data obtained for the sodium salt. The results are shown in Table 7. It is clear that, as seen in the previous analysis, a rigid isotropic model is inappropriate. The fits to the isotropic model have R values of more than 40% and predict a substantial field dependence for T_1 which is not observed experimentally. For the two state jump model, much better fits to the experimental data are observed, as seen by a 4-fold reduction in the R factor. The derived values of the motional parameters indicate that in methanol thyroxine sodium salt tumbles with an overall correlation time of 0.7 ns, but that superimposed on this motion is a faster internal motion ($\tau_i = 0.10$ ns) that can be represented by the aromatic rings jumping ±55° between the two conformers. While the NMR data fit this model to an accuracy approaching experimental error, (the R values are 4−11%), there may well be other models for the internal motion which would also provide an acceptable solution, i.e. the fit to this model does not guarantee that it is the only possible interpretation. It is clear from the NMR data, however, that models which do not incorporate internal motion are inappropriate. The results show unequivocally that there is a substantial degree of restricted amplitude internal motion in both rings of the thyroid hormones. This is confirmed by the model-free approach, which predicts overall and internal correlation times similar to those predicted by the two state jump model (Table 7).

Altering solution viscosity has the potential to modulate the relative rates of overall and internal motions; therefore, additional measurements were made in DMSO. Increasing the solution viscosity was expected to slow

Table 8. ^{13}C T_1s, $^{13}C\{^1H\}$ NOEs, and Chemical Shifts of the Hydrogen-Bearing Carbons of T4 in DMSO[a]

	^{13}C T_1 (s)[b]		$^{13}C\{^1H\}$ NOE[c]		chemical shifts
	75 MHz	125 MHz	75 MHz	125 MHz	(ppm)
C2′,6′	0.219 ± 0.003	0.273 ± 0.012	1.94 ± 0.02	1.60 ± 0.03	125.0
C2,6	0.214 ± 0.004	0.253 ± 0.011	2.01 ± 0.05	1.70 ± 0.10	140.8
Cα	0.249 ± 0.005	0.337 ± 0.005	2.10 ± 0.08	1.96 ± 0.12	54.9
Cβ	0.290 ± 0.026	0.330 ± 0.036	1.92 ± 0.16	1.74 ± 0.05	35.1

[a] Data were obtained at 306.5 K using a 26 mM solution. [b] Values are the average ± standard deviation of four (75 MHz) and five (125 MHz) T_1 experiments. [c] Values are the average ± standard deviation of four NOE experiments.

Table 9. Theoretical ^{13}C T_1s and $^{13}C\{^1H\}$ NOEs Fitted to T4 in DMSO Data

Isotropic Motion

	^{13}C T_1 (s)		$^{13}C\{^1H\}$ NOE			
	75 MHz	125 MHz	75 MHz	125 MHz	R (%)	τ_o (ns)
C2′,6′	0.16	0.22	2.23	1.77	18.6	0.50
C2,6	0.16	0.23	2.31	1.85	14.9	0.45
Cα	0.22	0.27	2.67	2.32	19.7	0.27
Cβ	0.17	0.24	2.44	1.99	27.5	0.39

Two-State Jump

	^{13}C T_1 (s)		$^{13}C\{^1H\}$ NOE						
	75 MHz	125 MHz	75 MHz	125 MHz	R (%)	τ_o (ns)	τ_i (ns)	β	θ
C2′,6′	0.20	0.29	1.94	1.64	4.2	0.75[a]	0.10	27	60[a]
C2,6	0.19	0.27	2.01	1.75	5.1	0.75[a]	0.20	28	60[a]
Cα	0.25	0.34	2.13	1.94	0.8	0.75[a]	0.18	37	60[a]
Cβ	0.39	0.51	2.18	2.03	29.0	0.75[a]	0.10	66	109.5[a]

Model-Free Approach

	^{13}C T_1 (s)		$^{13}C\{^1H\}$ NOE					
	75 MHz	125 MHz	75 MHz	125 MHz	R (%)	τ_o (ns)	τ_i (ns)	S
C2′,6′	0.20	0.29	1.94	1.64	4.2	0.75[a]	0.05	0.79
C2,6	0.19	0.27	2.01	1.75	5.1	0.75[a]	0.10	0.77
Cα	0.25	0.34	2.13	1.94	0.8	0.75[a]	0.09	0.64
Cβ	0.26	0.36	2.01	1.77	6.6	0.75[a]	0.05	0.67

[a] This parameter was fixed during iterative fitting.

the motions. Changing the solvent also gave the added benefit of increased solubility, allowing the measurements to be done at a higher concentration, significantly improving the signal-to-noise ratio and the quality of the data. T_1 and NOE data at 75 and 125 MHz for T4 in DMSO are given in Table 8. In contrast to the experimental data in methanol, there is now a significant dependence of the relaxation parameters on magnetic field strength, with T_1s increasing and NOEs decreasing with an increase in field strength. The theoretical parameters derived from fitting the three models to the experimental data in Table 8 are shown in Table 9. Once again, the models incorporating internal motion provide a much better fit to the experimentally observed results than the simple isotropic model, confirming that the thyroid hormones exhibit internal motion in DMSO. Both the two state jump model and the model-free approach predict the same overall correlation time and a similar internal rate of motion. Both models suggest that the outer ring moves more rapidly than the inner.

The side chain atoms Cα and Cβ also show some form of internal motion, as demonstrated by the fact that the isotropic model could not reproduce the experimental results. The nature of the motion, however, is unclear. It seems unlikely that the side chain would exhibit motion that could be described by the two state jump model, as there are too many combinations of rotations possible, and this is borne out by the results of the fits. The model-free approach fails to reproduce the experimental results also. For the data acquired at two different fields, the fits to the model-free approach are similar to those of the two state jump model (Table 9). The side chain clearly exhibits internal motion, but its exact nature is too complex to be identified.

Discussion

The motional parameters derived from the NMR relaxation data measured in this study clearly show that the thyroid hormones exhibit internal motion. The internal motion was modeled as rapid jumps of both aromatic rings between two equally favorable conformers superimposed on overall isotropic tumbling of the hormone. The derived value for the overall correlation time of T4 in methanol was 0.35 ns, a value consistent with that derived from the Stokes−Einstein equation[27] (using values of 0.51 cP for the solution viscosity at 30 °C, and an average molecular radius of 5 Å, an overall correlation time of 0.19 ns was obtained from this equation). The fact that the overall correlation time derived from the two state jump model is close to that based on the hydrodynamic properties of the hormones suggests that the model is reasonable and hence also likely to provide a good estimate of the internal motion. For T4 the internal motion was an order of magnitude faster than the overall correlation time, and the jump amplitude of the rings was approximately ±55°. T3 and T2 showed similar jump amplitudes but with slightly faster jump rates, likely due to these molecules having fewer iodines.

Examination of the internal motional parameters τ_i and β shows that in general the amplitude of the jumping motions is similar for the two rings, but the rates differ, with the outer ring showing the higher jump frequency. The faster motion of the outer ring appears to be due to the fact that the inner ring is substituted with an alanyl side chain, while the outer ring carries a much smaller hydroxyl group.

The rates of the overall and internal motion are affected by both the charge state of the molecule and the viscosity of the solvent. The salt of T4 in methanol and the free acid in DMSO showed increased overall and internal correlation times relative to the free acid in methanol. The ratio of the two correlation times was also reduced, indicating that for each reorientation of the molecule the rings jump between conformers less often compared to those of the free acid in methanol. The reduced mobility in DMSO is easily explained by the greater viscosity of the solvent, while the introduction of charge to the side chain would make motion less favorable energetically. Interestingly, the jump amplitude in DMSO was half that in methanol, perhaps too as a result of the increased solvent viscosity.

The ^{13}C T_1s of T3 sodium salt in DMSO have been reported previously[26] but at a lower magnetic field strength than was used here. At 25 MHz the T_1s of the hydrogen-bearing ring carbons were 0.063−0.065 s for the outer ring and 0.070 s for the inner. The concentration used was much higher than that of this work, making direct comparison of the data difficult; however, this low field data offers the potential of providing extra verification of the motional model used. If the internal motional parameters derived from the two state jump model for T4 in DMSO (see Table 9) are fixed while τ_o is allowed to vary, then the T_1s of Mazzocchi et al.[26] can be reproduced by an overall correlation time of 2.5 ns. Taking into account the fact that Mazzocchi et al. used the sodium salt, which we found to double τ_o relative to the free acid, and used a much more highly concentrated solution, which would also increase the correlation time (and potentially the internal correlation time also), this value is consistent with our value for the overall correlation time. The two state jump model predicts an NOE of 1.80 at 25 MHz, but Mazzocchi et al. did not report any NOEs which could be used to more stringently test the model of motion. In general, though, the previously reported T_1s for T3 are consistent with the motional model reported here.

The parameters derived from the two state jump model in DMSO are in good agreement with the equilibrium conformation found in crystal structures of a range of hormone analogues.[1] The crystal structures show that ϕ and ϕ' (defined in Figure 1) fall into two classes, namely $\phi = 108°$, $\phi' = -28°$ and $\phi = -108°$, $\phi' = 28°$. As the jump axes are simply an extension of the diphenyl ether linkage through each ring, the torsion angles in the crystal structure can be related directly to β. A value of $\pm 108°$ for ϕ corresponds to $\beta = 18°$ for the inner ring, while $\phi' = \pm 28°$ is equivalent to $\beta = 28°$ for the outer ring. In DMSO the jump angle of the outer ring is in excellent agreement with the angle observed in the crystal structures, while the jump angle of the inner ring is slightly larger.

The NMR relaxation data in this study have been used to identify internal motion of the thyroid hormones

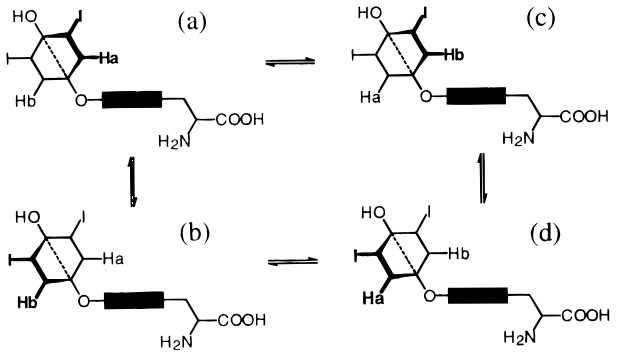

Figure 5. Schematic illustration of motions of the outer ring of T4. The dotted line through the outer ring shows the jump axis about which the ring rotates. (a) Ha is shown in the proximal position and is closer to the viewer than Hb due to the torsion angle ϕ' being greater than 0°. This conformation corresponds to one of the two states of the two state jump model and agrees with the "twist" of the outer ring observed in the crystal structure of T4. (b) Rotation about the dotted line through the center of the outer ring has moved Ha away from the viewer and brought Hb toward the viewer. This corresponds to the second state of the outer ring in the two state jump model. (c) Hb is now in the proximal position and closer to the viewer than Ha. (d) Hb is in the proximal position and is now further from the viewer than Ha. Transition from a to b and from c to d involves small amplitude jumps on the nanosecond time scale and is detected by NMR relaxation measurements. Although not illustrated in this figure, the inner ring also exhibits this type of motion. Transitions a to c and b to d result in a 180° flip of the outer ring and exchange of the environments of Ha and Hb. This ring flip occurs on a microsecond time scale and is detected by variable temperature studies.

on the nanosecond time scale. Previous variable temperature line shape measurements[9] have characterized internal motion on the microsecond time scale which was subsequently modeled to identify the most likely pathway for interconversion of the H2′ and H6′ protons.[18] A unified model describing all of the internal motions of the thyroid hormones can now be proposed (Figure 5). In this model, both aromatic rings of the thyroid hormones jump rapidly between two energetically equivalent conformations on a nanosecond time scale (a ↔ b and c ↔ d in Figure 5). The half-angle of the jump varies between 27° and 55°, depending on the solvent, corresponding to an average displacement of about 90° between the two extreme jump positions. These separate states are not detectable on the chemical shift time scale but lead to an average proximal environment for Ha and an average distal environment for Hb (due to rapid interchange between a and b in Figure 5), which are seen in the low temperature spectra. However, these fast motions are detected by relaxation studies. While the rate of this motion is rapid, its amplitude is not sufficient to average the environment of proximal and distal protons. Occasionally (about once every 1000 jumps) the outer ring jumps further than the nominal 90° range, exchanging the environments of the proximal and distal protons (a ↔ c and b ↔ d in Figure 5). While the actual rate of an individual ring flip is rapid, the effective rate of the process is on the microsecond time scale, because on average a large number of small amplitude jumps occur for every large amplitude ring flip. It is the exchanging of proximal and distal protons on the microsecond time scale that is detected by the variable temperature line shape studies.

The fact that thyroxine and the other thyroid hormones are able to so freely move over a moderately large region of conformational space has implications for receptor binding. The recent crystal structure of the thyroid receptor ligand binding domain complexed with the thyroid agonist 3,5-dimethyl-3′-isopropylthyronine[16] shows that the thyroid hormones bind at the center of the hydrophobic core of the ligand binding domain and may play a structural role in the conformational changes which activate the receptor. The structures of the retinoid-X receptor ligand binding domain[23] and the retinoic acid−retinoic acid receptor ligand binding domain complex[22] indicate that significant conformational changes accompany ligand binding. The conformational flexibility shown by the thyroid hormones may be required for binding. The rapid "wiggling" of the aromatic rings could enable the hormone to work its way to the center of the ligand binding domain as the protein reorders itself about the ligand and may in fact trigger the conformational changes.

Experimental Section

Thyroxine, 3,5,3′-triiodothyronine, 3,5-diiodothyronine, and thyroxine sodium salt were obtained from Sigma. Methanol-d_4 (99.8%) and DMSO-d_6 (99.96%) were obtained from Cambridge Isotope Laboratories. Methanol solutions were saturated (∼1 mM for the free acids and ∼10 mM for the salt), while the DMSO solution was 26 mM. All solutions were degassed prior to recording proton data. Initially the solutions were degassed when acquiring ^{13}C data also, but it was found not to affect the results, so further experiments were recorded without degassing. Data were recorded on Bruker AMX-300 and 500 instruments at 306.5 K using 10 mm tubes for the ^{13}C experiments and 5 mm for the proton. The fast inversion recovery pulse sequence[39] was used. Spectra were referenced to solvent signals, either methanol (^1H 3.30 ppm and ^{13}C 49.0 ppm) or DMSO (^{13}C 39.5 ppm). Relaxation rates were determined from a three parameter exponential fit to the data using either the standard Bruker routine or Microsoft Excel. Experimental data were fitted to models of motion using the program MOLDYN running on a VAX 3400. All fits were performed with the bond length set to 1.09 Å. The best fits were obtained when only two parameters at a time were allowed to vary. Thus, an initial fit in which all parameters were varied was used to determine an average value for τ_o. τ_o was then stepped through a series of fixed values close to the average while the other two variable parameters were iteratively fitted. Initial guesses for τ_i, β, and S were 0.1 ns, 30°, and 1, respectively, and the ratio of the lifetimes of the two states for the two state jump model was set to 1.

Acknowledgment. This work was supported in part by a grant from the Australian Research Council (D.J.C., Australian Senior Research Fellowship).

References

(1) Cody, V. Thyroid Hormone Interactions: Molecular Conformation, Protein Binding and Hormone Action. *Endocr. Rev.* **1980,** *1*, 140−166.
(2) Oppenheimer, J. H. Thyroid hormone action at the molecular level. In *Werner and Ingbar's The Thyroid*, 6th ed.; Braverman, L. E., Utiger, R. D. Eds.; J. B. Lippincott: Philadelphia, 1991; pp 204−224.
(3) Craik, D. J.; Duggan, B. M.; Munro, S. L. A. Conformations and binding interactions of thyroid hormones and analogues. In *Studies in Medicinal Chemistry, Volume 2 Biological Inhibitors*, 1st ed.; Choudhary, M. I. Ed.; Harwood: Amsterdam, 1996; pp 255−302.
(4) Jorgensen, E. C. Thyroid Hormones and Analogs. II. Structure−Activity Relationships. In *Hormonal Proteins and Peptides*, 1st ed.; Li, C. H. Ed.; Academic Press: New York, 1978; pp 107−204.
(5) Andrea, T. A.; Dietrich, S. W.; Murray, W. J.; Kollman, P. A.; Jorgensen, E. C. A Model for Thyroid Hormone-Receptor Interactions. *J. Med. Chem.* **1979**, *22*, 221−232.
(6) Somack, R.; Andrea, T. A.; Jorgensen, E. C. Thyroid Hormone Binding to Human Serum Prealbumin and Rat Liver Nuclear Receptor: Kinetics, Contribution of the Hormone Phenolic Hydroxyl Group, and Accommodation of Hormone Side-Chain Bulk. *Biochemistry* **1982**, *21*, 163−170.
(7) Lehman, P. A.; Jorgensen, E. C. Thyroxine Analogs. XIII. NMR evidence for hindered rotation in diphenyl ethers. *Tetrahedron* **1965**, *21*, 363−380.
(8) Emmett, J. C.; Pepper, E. S. Conformation of Thyroid Hormone Analogues. *Nature* **1975**, *257*, 334−336.
(9) Gale, D. J.; Craik, D. J.; Brownlee, R. T. C. Variable Temperature NMR Studies of Thyroid Hormone Conformations. *Magn. Reson. Chem.* **1988**, *26*, 275−280.
(10) Cody, V.; Duax, W. L.; Norton, D. A. Molecular conformation of the thyroxine analogue 3,5-diiodo-L-thyronine *N*-methylacetamide complex (1:1). *Acta Crystallogr.* **1972**, *B28*, 2244−2252.
(11) Cody, V. Crystal structure and molecular conformation of the thyroid hormone distal 3,5,3′-triiodo-L-thyronine. *J. Am. Chem. Soc.* **1974**, *96*, 6720−6725.
(12) Camerman, A.; Camerman, N. Thyroid hormone stereochemistry. I. The molecular structures of 3,5,3′-triiodo-L-thyronine (T3) and L-thyroxine (T4). *Acta Crystallogr.* **1974**, *A30*, 1832−1840.
(13) Fawcett, J. K.; Camerman, N.; Camerman, A. Thyroid hormone stereochemistry. IV. Molecular conformation of 3′-isopropyl-3,5-diiodo-L-thyronine in the crystal and in solution. *J. Am. Chem. Soc.* **1976**, *98*, 587−591.
(14) Mazzocchi, P. H.; Ammon, H. L.; Colicelli, E.; Hohokabe, Y.; Cody, V. NMR studies of triiodothyropropionic acid in ethanol-HCl. *Experientia* **1976**, *32*, 419−420.
(15) Jorgensen, E. C.; Lehman, P. A.; Greenberg, C.; Zenker, N. Thyroxine Analogues. VII Antigoitrogenic, calorigenic and hypocholesteremic activities of some aliphatic, alicyclic, and aromatic ethers of 3,5-diiodotyrosine in the rat. *J. Biol. Chem.* **1962**, *237*, 3832−3838.
(16) Wagner, R. L.; Apriletti, J. W.; McGrath, M. E.; West, B. L.; Baxter, J. D.; Fletterick, R. J. A structural role for hormone in the thyroid hormone receptor. *Nature* **1995**, *378*, 690−697.
(17) Andrews, P. R.; Craik, D. J.; Munro, S. L. A. The relationship between NMR, X-ray and theoretical methods of conformational analysis: application to thyroid hormones. In *NMR spectroscopy in drug research*, 1st ed.; Jaroszewski, J. W., Schaumburg, K., Kofod, H., Eds.; Munksgaard: Copenhagen, 1988; pp 20−39.
(18) Craik, D. J.; Andrews, P. R.; Border, C.; Munro, S. L. A. Conformational studies of thyroid hormones. I. The diphenyl ether moiety. *Aust. J. Chem.* **1990**, *43*, 923−936.
(19) Clore, G. M.; Gronenborn, A. M.; Birdsall, B.; Feeney, J.; Roberts, G. C. K. ^{19}F-n.m.r. studies of 3′,5′-difluoromethotrexate binding to *Lactobacillus casei* dihydrofolate reductase. *Biochem. J.* **1984**, *217*, 659−666.
(20) Cheung, H. T. A.; Searle, M. S.; Feeney, J.; Birdsall, B.; Roberts, G. C. K.; Kompis, I.; Hammond, S. J. Trimethoprim binding to *Lactobacillus casei* dihydrofolate reductase: A ^{13}C NMR study using selectively ^{13}C-enriched trimethoprim. *Biochemistry* **1986**, *25*, 1925−1931.
(21) Searle, M. S.; Forster, M. J.; Birdsall, B.; Roberts, G. C. K.; Feeney, J.; Cheung, H. T. A.; Kompis, I.; Geddes, A. J. Dynamics of trimethoprim bound to dihydrofolate reductase. *Proc. Nat. Acad. Sci. U.S.A.* **1988**, *85*, 3787−3791.
(22) Renaud, J.; Rochel, N.; Ruff, M.; Vivat, V.; Chambon, P.; Gronemeyer, H.; Moras, D. Crystal structure of the RAR-γ ligand-binding domain bound to all-trans retinoic acid. *Nature* **1995**, *378*, 681−689.
(23) Borguet, W.; Ruff, M.; Chambon, P.; Gronemeyer, H.; Moras, D. Crystal structure of the ligand binding domain of the human nuclear receptor RXR-α. *Nature* **1995**, *375*, 377−382.
(24) Evans, R. M. The steroid and thyroid hormone receptor superfamily. *Science* **1988**, *240*, 889−895.
(25) Ong, R. L.; Pittman, C. S. Proton nuclear magnetic resonance assignments of thyroid hormone and its analogues. *Biochem. Int.* **1985**, *5*, 803−811.
(26) Mazzocchi, P. H.; Ammon, H. L.; Colicelli, E. Carbon-13 NMR Studies of Thyroid Hormones and Model Compounds. The Conformational Analysis of Diphenyl Ethers. *Org. Magn. Reson.* **1978**, *11*, 143−149.
(27) London, R. E. Intra molecular dynamics of proteins and peptides as monitored by nuclear magnetic relaxation measurements In *Magnetic resonance in biology*, 1st ed.; J. S, Cohen Ed.; John Wiley and Sons: New York, 1980; pp 1−69
(28) Craik, D. J.; Levy, G. C.; Kumar, A. MOLDYN: A generalized program for the analysis of NMR spin-relaxation data. *J. Chem. Inf. Comput. Sci.* **1983**, *23*, 30−38.
(29) Brainard, J. R.; Szabo, A. Theory for nuclear magnetic resonance relaxation of probes in anisotropic systems: application to

cholesterol in phospholipid vesicles. *Biochemistry* **1981**, *20*, 4618−4628.
(30) Howarth, O. W. Effect of internal librational motions on the ^{13}C nuclear magnetic resonance relaxation times of proteins and peptides. *J. Chem. Soc., Faraday Trans. 2* **1978**, *74*, 1031−1041.
(31) Lipari, G.; Szabo, A. Nuclear magnetic resonance relaxation in nucleic acid fragments: models for internal motion. *Biochemistry* **1981**, *20*, 6250−6256.
(32) London, R. E. On the interpretation of ^{13}C spin−lattice relaxation resulting from ring puckering in proline. *J. Am. Chem. Soc.* **1978**, *100*, 2678−2685.
(33) London, R. E.; Phillippi, M. A. A ^{13}C NMR study of the solution dynamics of 1,3,5,-triphenylbenzene; Analysis of motion about the phenyl−phenyl bond. *J. Magn. Reson.* **1981**, *45*, 476−489.
(34) Richarz, R.; Nagayama, K.; Wuthrich, K. Carbon-13 nuclear magnetic resonance relaxation studies of internal mobility of the polypeptide chain in basic pancreatic trypsin inhibitor and a selectively reduced analogue. *Biochemistry* **1980**, *19*, 5189−5196.
(35) Wang, C. C.; Pecora, R. Time-correlation functions for restricted rotational diffusion. *J. Chem. Phys.* **1980**, *72*, 5333−5340.
(36) Woessner, D. E.; Snowden, B. S.; Meyer, G. H. Nuclear spin−lattice relaxation in axially symmetric ellipsoids with internal motion. *J. Chem. Phys.* **1969**, *50*, 719−721.
(37) Lipari, G.; Szabo, A. Model-free approach to the interpretation of nuclear magnetic resonance relaxation in macromolecules. 1. Theory and range of validity. *J. Am. Chem. Soc.* **1982**, *104*, 4546−4559.
(38) Lipari, G.; Szabo, A. Model-free approach to the interpretation of nuclear magnetic resonance relaxation in macromolecules. 2. Analysis of experimental results. *J. Am. Chem. Soc.* **1982**, *104*, 4559−4570.
(39) Vold, R. L.; Waugh, J. S.; Klein, M. P.; Phelps, D. E. Measurement of spin relaxation in complex systems. *J. Chem. Phys.* **1968**, *48*, 3831−3832.

JM960231+